2006-01-0808

Aerodynamics for Formula SAE: A Numerical, Wind Tunnel and On-Track Study

Scott Wordley and Jeff Saunders
Monash Wind Tunnel, Mechanical Engineering
Monash University

ABSTRACT

The detail design and development of a high downforce aerodynamics package for a Formula SAE car is described. Numerical methods are first used to develop multi-element wing profiles which conform to FSAE rules while still generating high negative lift coefficients. A range of full scale wind tunnel testing data is presented for these designs, demonstrating their performance, both in isolation (free-stream), and on the car. Three different techniques are also developed for measuring the performance of a front wing in ground effect.

INTRODUCTION

This work is the second in a series of papers which summarize the four year design and development of a high downforce aerodynamics package for the 2003 Monash University Formula SAE car. A companion paper by the same authors [1] covers rule considerations and the process of initial design specification. An aerodynamically balance wing package was designed to produce maximum downforce within the stated acceptable limits of increased drag and reduced top speed. The net effect of these wings on the car's performance in the Formula SAE Dynamic Events was then predicted. The addition of the wing package described showed the potential for significantly improved cornering and braking with only slightly diminished straight line acceleration.

This paper will document the detail design and testing process for this wing package.

A computational fluid dynamics (CFD) package was first used to develop 2-dimensional wing profiles to achieve the target lift and drag coefficients specified in [1]. A range of profiles from the literature were trialed and then modified to comply with Formula SAE leading and trailing edge rules. Studies of slot gap geometry, angle of attack and ground effect were used to decide on the front and rear wing profiles which were then built for wind tunnel testing.

The prototype wings were then tested using a number of different methods in the Monash Full Scale Wind Tunnel. 'Free-stream' testing of both wings was used to correlate with CFD data and allow fine tuning of slot gap geometry. A study of the height sensitivity of the rear wing on the car was completed to determine the best compromise between increased downforce (high mount) and low centre of gravity height (low mounting).

Due to the lack of an existing 'moving-ground' simulation in the wind tunnel, techniques were developed to quantify and tune the performance of the front wing in 'ground effect'.

A pressure tapped front wing was constructed and pressures logged at a total of 128 points on the wing. This data was used to develop surface pressure contour plots, which, when integrated, gave an estimate of the resultant forces for download and drag. A validation study was conducted in the wind tunnel to document the accuracy of the procedure, with a view to using it for on-track tests of the wing in ground effect.

A 'symmetrical plane' test method was also trialed, where the front half of the Formula SAE car was mirrored in full scale, in a horizontal plane 1.5 m above the ground. This allowed the effect of a 'moving ground' to be approximated by the development of a flow streamline in this plane.

Finally, a strain gauged, unsprung mounting system was built to log the downforce generated by the front wing whilst driving on track. These mounts also allowed considerable adjustment of the wing ride height and wing angle of attack. A pitot tube was used to account for variations in the natural wind.

CFD ANALYSIS

Formula SAE rules [2] state that all 'wings' and wing elements must feature leading edge radii of at least 12.7mm (1/2") and trailing edge radii of at least 3mm (1/8"); a criteria which eliminates virtually all pre-existing wing profiles [3] which sensibly make use of a sharp

trailing edge to maximize pressure recovery. This rule has serious implications for slot gap geometry which is crucial for the performance of a multi-element, high-lift wing. In order to comply with these rules while maintaining high lift coefficients, new profiles were designed and tested using the Fluent CFD package.

CFD DESCRIPTION AND VALIDATION

The accuracy of this two dimensional CFD package for predicting the performance of wings was first validated against the wind tunnel data of Zhang and Zerihan [7] for an isolated two element wing in ground effect. These profiles and an example of the two dimensional mesh is shown in Figure 1 below. The results of these CFD tests are given in Figure 2, where the lift and drag coefficients are plotted as a function of ground clearance, which is expressed as a proportion of chord length.

The closeness of this comparison gave an acceptable level of confidence in the accuracy of the numerical modeling.

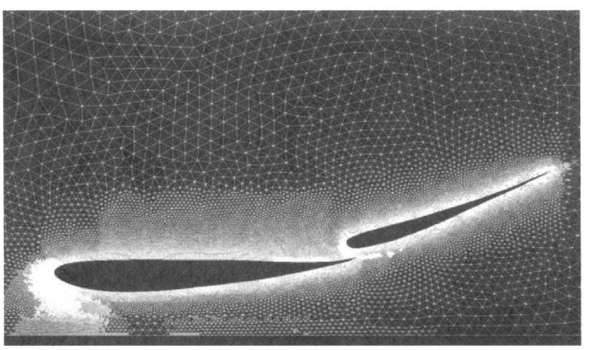

Figure 1: Wing profiles (after Zhang and Zerihan [7]) and example mesh for moving ground 2D CFD validation study.

INITIAL PROFILE DESIGN

Wordley and Saunders [1] identify target lift coefficients of 3.4 and 3.5 for front and rear wings respectively. A review of the literature [3, 4, 5] suggested that such high coefficients are only achievable with multi-element profiles. Following the multi-element design recommendations of McBeath [4], a three-element front wing and five-element rear wing was specified. To simplify the manufacturing process, both wings were designed to make use of the same flap profile. Gurney flaps (3% front and 4% rear chord) are used on the rear most flaps of both wings. These profiles along with the two dimensional CFD meshes used are shown in Figures 3 and 4 below.

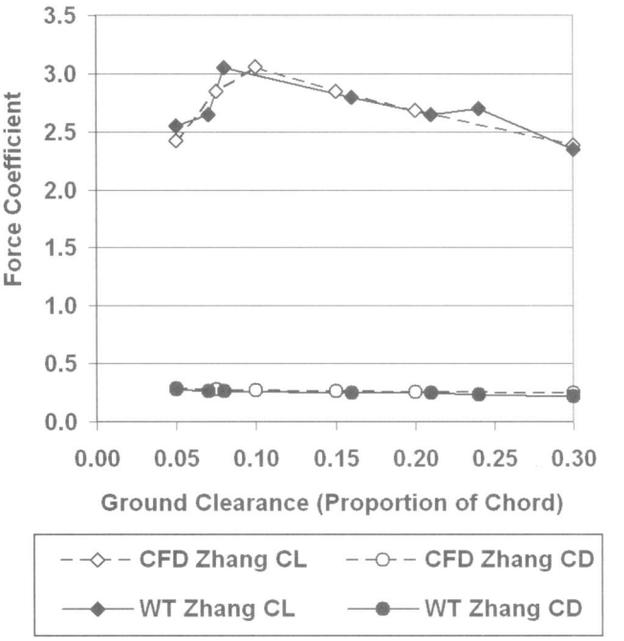

Figure 2: 2D CFD versus 3D wind tunnel measurements for a two element wing in ground effect (CFD chord length: 420 mm, Re: 0.50 x 10^6, experimental data from [7]).

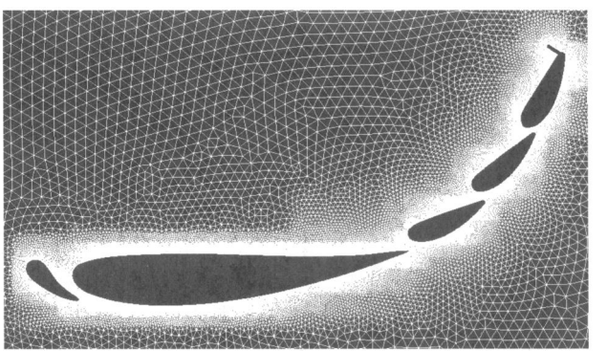

Figure 3: Rear wing profiles and mesh for free-stream 2D CFD

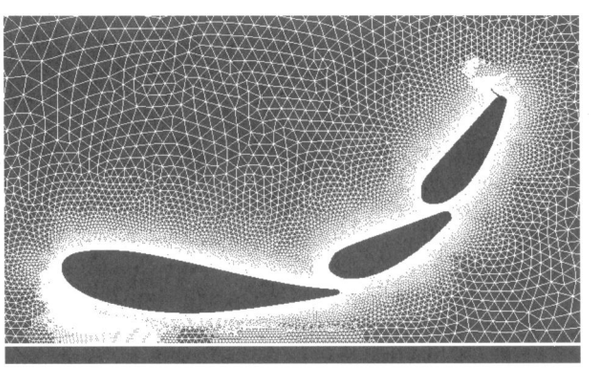

Figure 4: Front wing profiles and mesh for ground effect 2D CFD,

2D CFD FRONT WING ANALYSIS

Front Wing in 'Free-stream' Results

The performance of the front wing in free-stream air flow was predicted using two dimensional CFD. The force coefficients versus angle of attack determined from numerical modelling are shown below (Fig. 5).

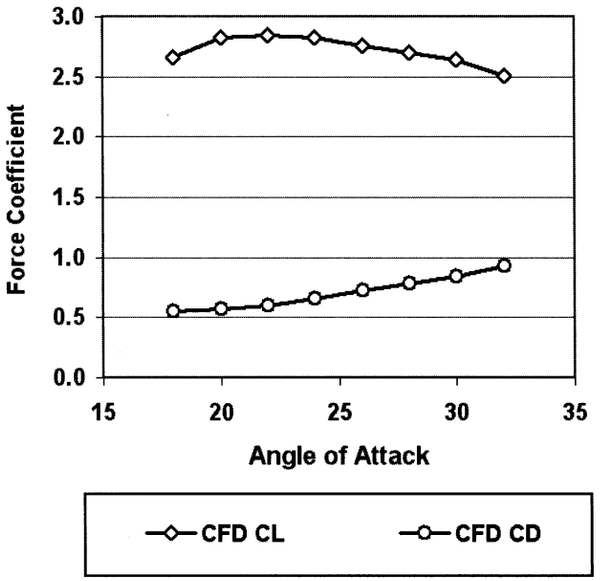

Figure 5: 2D CFD predicted force coefficients for the 3 element front wing in free-stream flow versus angle of attack (chord length: 420 mm, Re: 0.50 x 10^6)

Beyond 22 degrees angle of attack a gradual trailing edge stall was predicted, starting at the rear most flap. By 32 degrees, the CFD predicted separated flow on the underside of both flap elements, but attached flow for the underside of the main plane.

Front Wing in 'Ground Effect' Results

Using two-dimensional CFD, the same wing was then numerically modeled with a simulated moving ground plane for a range of different ground clearance heights and angles of attack. A graph of the force coefficients obtained from these tests is shown in Figure 6.

These results show how the lift coefficient achieved by this profile is dependant on a complicated interaction between ground clearance and angle of attack. Larger wing angles of attack appear more sensitive to ground clearance. Drag is seen to stay reasonably constant with change in ground clearance, but increases significantly with higher angles of attack. While it would have been interesting to model larger ground clearances, they were neglected in this study because of packaging considerations.

Compared to the profiles tested by Zhang (which do not comply with FSAE rules), this design incurs a much higher drag penalty but is able to achieve the higher target lift coefficients specified in the initial design.

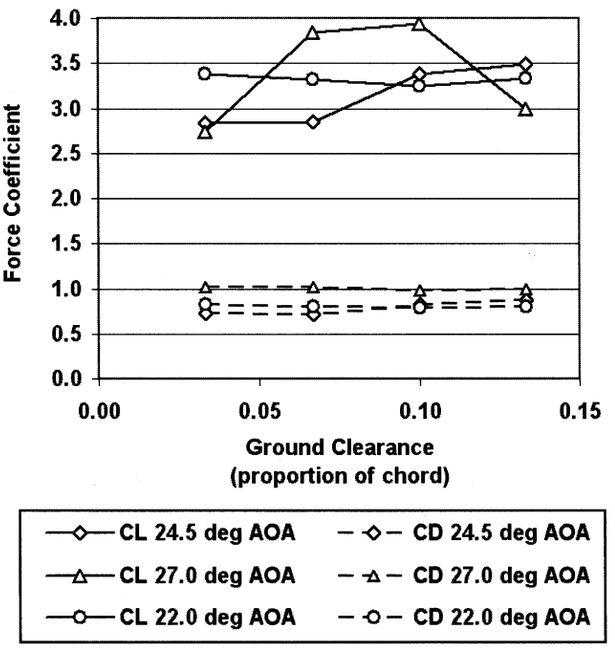

Figure 6: Front wing in ground effect force coefficients for a range of angles of attack, versus ground clearance (chord length: 420 mm, Re: 0.50 x 10^6).

2D CFD REAR WING ANALYSIS

The performance of the rear wing in free-stream air flow was also predicted using 2D CFD. The force coefficients versus angle of attack determined from numerical modelling are shown in Figure 7.

The CFD results predicted that this wing would achieve the target lift coefficient of 3.5 at an angle of attack of 31 degrees. At higher angles of attack a gradual trailing edge separation on the rear most flap was predicted, with downforce steadily decreasing and drag increasing beyond this angle.

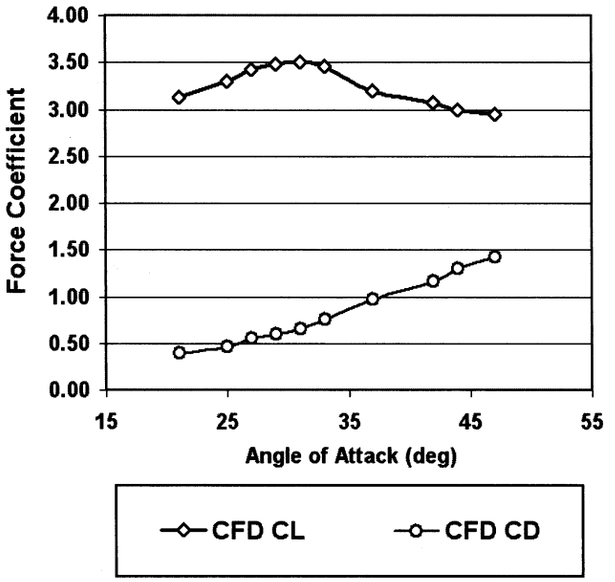

Figure 7: 2D CFD predicted rear wing in free stream force coefficients versus angle of attack (chord length: 815 mm, Re: 0.5 x 10^6).

3D FULL CAR ANALYSIS

Some time ago (in 2002), a post-graduate team member (Shaun Johnson) performed a small number of 3-dimensional, full-car, CFD tests. These tests were used to make a preliminary assessment of wing and car interactions and to design cooling ducts and underbody diffusers for the 2002 Monash FSAE vehicle.

The 3D CFD model used symmetry along the car centerline, in order to reduce the total grid count by half. The flow inlet plane was located two car lengths upstream of the model and the outlet plane four car lengths downstream of the model. The side boundaries were located sufficiently far from the model to minimize blockage effects. A moving ground plane and rolling wheels were simulated. A hybrid mesh was employed, which used prisms on the critical surfaces and tetrahedrals to fill out the rest of the domain. In total, around 2 million cells were used.

The Gambit software package was used to pre-process the model geometry. A Kω-SST turbulence model was used, and the lift and drag forces on the body were set as convergence criterions. Running on a single workstation and using a commercial Fluent license, each case took several days to solve.

A sample of the results is shown in Figures 8 and 9 below.

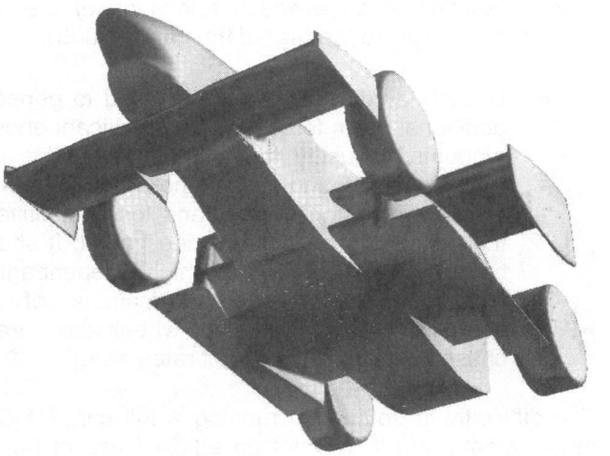

Figure 8: Full car 3D CFD example results for the 2002 Monash vehicle, underside view, shaded for pressure (Best grey scale picture available).

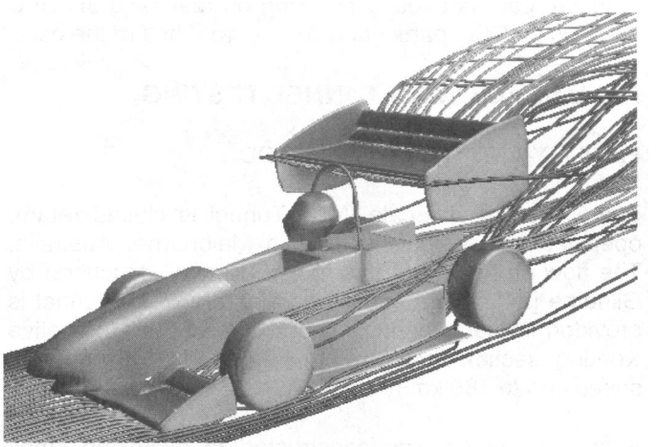

Figure 9: Full car 3D CFD example results for the 2002 Monash vehicle, car shaded for pressure, streamlines shaded for velocity.

This limited study suggested that:

- The performance of the front wing was adversely affected by the nose and front wheel interaction, with down force reduced by around 35%.
- The performance of the rear wing was adversely affected by the car and the driver helmet, with downforce reduced by around 30%.
- The majority of the cooling airflow was deflected above the inlets to the side mounted heat exchangers. This finding prompted further investigation of cooling system performance using the specific dissipation technique [10], and

resulted in an eventual relocation of the heat exchanger to the rear of the car (in 2005).

- Underbody diffusers could be used to generate additional down force, but not significant enough amounts to justify their inclusion on this car. Wings were found to be more efficient on a weight / downforce basis and less sensitive to the expected variations in ride height. It should be noted that this finding is highly dependant on the dimensions and specifications of the particular car (including wheelbase, track, chassis size, wheel and roll rates etc).

The difficultly in setting up running a full car, 3D CFD model meant that it was not an efficient use of human resources for the Monash team, given our access to a full scale tunnel. For this reason it was decided to generally limit our CFD research to 2D wing profile work and concentrate on the experimental testing described later in this paper. However, the steady improvement CFD programs and computer processing power is making full car simulations increasingly attractive. The Monash team is already planning on resuming 3D CFD analysis in 2006, particularly for the front half of the car.

FULL SCALE WIND TUNNEL TESTING

FACILITY AND TESTING METHOD

The Monash Full Scale Wind Tunnel is closed return, open jet wind tunnel, located in Melbourne, Australia. The flow properties of this tunnel are well described by Gilhome [24], and a schematic diagram of the tunnel is provided in the Appendix. The nozzle of the automotive working section is 2.6m by 4.0m and is capable of speeds up to 180 km/h.

A specialized rig was constructed to allow the small wheelbase and track Formula SAE car to be mounted to the tunnel balance. This rig was also designed to allow wings to be held and tested (with endplates) in 'free-stream' flow with no car in place. These tests were used to understand and tune the performance of the wings in isolation from the car, and will be examined first. The minor amount of drag and lift generated by the rig itself was subtracted from all results.

WINGS IN 'FREE-STREAM' TESTING

Front Wing Tests

The lift and drag coefficients, measured in the wind tunnel, for the front wing in free-stream are shown in Figure 7 below. The CFD predictions are provided on the same graph for comparison.

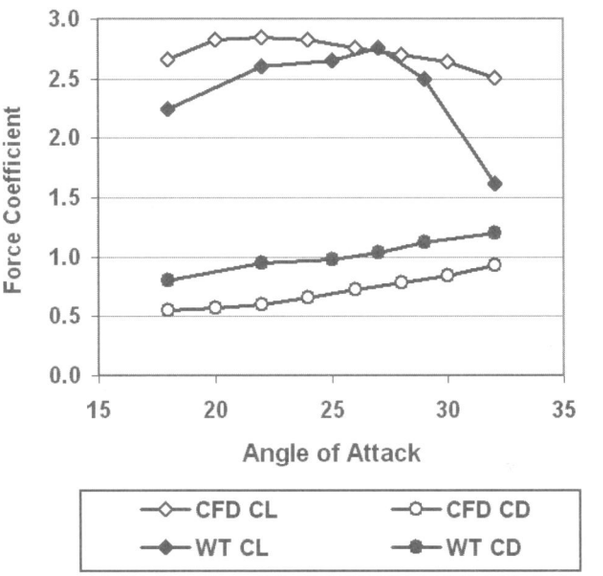

Figure 7: Front wing in free-stream, measured wind tunnel force coefficients versus angle of attack, AR: 3.33 (2D CFD results shown for comparison).

The wind tunnel tests achieved a similar maximum lift coefficient (2.7) to that predicted by CFD but at a higher angle of attack. This was attributed to the effect of the small aspect ratio (3.33) compared to the 2D CFD which assumes an infinite aspect ratio. In the wind tunnel, the front wing was found to begin stalling at 29 degrees angle of attack. Smoke visualisation at this setting indicated that the flow had separated on the underside of the rear-most flap. Further increasing this angle of attack resulted in a leading edge separation at 32 degrees, and a corresponding large decrease in downforce. The measured drag was substantially higher than that predicted by 2D CFD, most likely due to induced drag which is not accounted for in the CFD results.

Rear Wing Tests

The lift and drag coefficients, measured in the wind tunnel, for the rear wing in free-stream are shown in Figure 8 below. The CFD predictions are provided on the same graph for comparison.

The wind tunnel results showed a trailing edge separation on the rear most flap beginning at 38 degrees. By 40 degrees the underside of this flap was fully separated, resulting in a plateau in the CL curve. The flow on the underside of the main plane remained attached until 48 degrees, beyond which a complete leading edge separation was observed. The considerable difference between the stall angles predicted by CFD and measured in the wind tunnel was most likely due to the extremely small aspect ratio of the

wind tunnel tested wing (1.72). Again, the wind tunnel drag is believed to be higher than predicted from CFD due to induced drag. It is interesting to note that further testing showed that removal of the leading edge slat reduced the maximum CL angle of attack of this wing by 8 degrees and decreased the maximum lift coefficient by 0.2 CL.

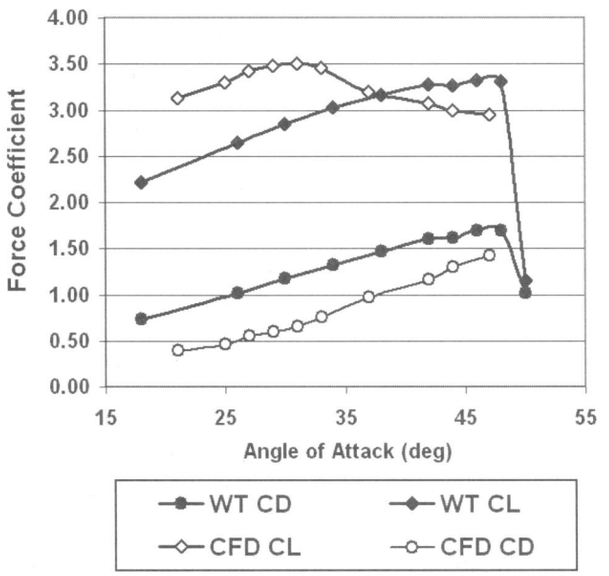

Figure 8: Rear wing in free-stream, measured wind tunnel force coefficients versus angle of attack, AR: 1.72 (2D CFD results shown for comparison)

Because the downforce is needed most when a race car is turning a corner it is important to check the sensitivity of a wing to yaw angle. A graph of force coefficients for the rear wing only, versus wind yaw angle is shown in Figure 9. Around 90% of the maximum downforce is retained out to a yaw angle of 20 degrees, which is an excessive amount of yaw for most formulas, but likely to be experienced by Formula SAE cars which negotiate tight tracks with very low speed corners. In order to increase the amount of downforce retained at high yaw angles, the leading edge of the endplate was radiused (12mm radius) to try and keep the flow attached on the leeward side of the endplate at high yaw angles. The resulting change in CL due to this modification is shown in Figure 9, with a significant increase in downforce between 25 and 40 degrees yaw. On-track, cobra-probe logging of wind yaw angle will be used to document a realistic yaw angle operating range to determine if this modification is warranted.

The coefficient of side force for the rear wing is also plotted versus yaw in Figure 9. The wing endplate, which presents an increasingly bluff surface when yawed, is the major source of this force. Given design freedom (as in this formula), endplate sizing is therefore a complicated task given that:

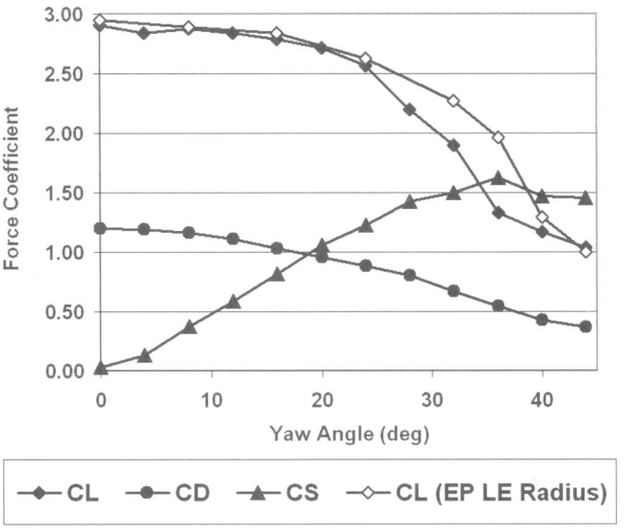

Figure 9: Rear wing in free-stream, measured wind tunnel force coefficients versus yaw angle attack, AR: 1.72. Endplate size 0.8m wide by 0.7m high.

- In general, increasing endplate size increases the downforce generated by a wing, improving both the vehicle's yaw acceleration and steady state cornering.
- For a rear wing, the endplates will develop a side force and yawing moment which will have a stabilizing effect on the car, in that the side force generated will oppose the prevailing attitude of the car, be it over-steer or under-steer.
- For a front wing, the endplates will develop a side force and yawing moment which will have a destabilizing effect on the car, in that the side force generated will act to increase the prevailing attitude of the car, be it over-steer or under-steer.
- All endplates are sensitive to gusts and side winds which may make the handling of the car unpredictable.

For this reason the Monash FSAE team has gathered a large set of wind tunnel data specifically relating to rear wing endplate size and shape. On-track testing and data logging with different size and shaped rear wing endplates will be used to determine the best compromise between high downforce and reduced yawing moment.

WINGS 'ON-CAR' TESTING

Base Car Tests

The table below lists the wind tunnel measured values of drag and lift for both the base car (with driver) and also the car and driver with the front wing fitted. The front wing was seen to increase the drag of the base car by around 14%. The wind tunnel measured downforce for the car with the front wing was around 40% less than expected on-track due to the lack of a moving ground simulation.

Car Configuration	CL	CD	Frontal Area (m^2)
Base Car (with Driver)	0.15	0.83	0.9
Car + Front Wing (with Driver)	-1.00	0.95	0.9

Rear Wing Height Sensitivity

To measure the effect that the front wing, vehicle and driver has on the performance of the rear wing, the car was correctly positioned with respect to the rear wing but isolated from the force balance system. Using this set-up, the rear wing was tested at a range of different heights to understand this interaction (See Fig. 10).

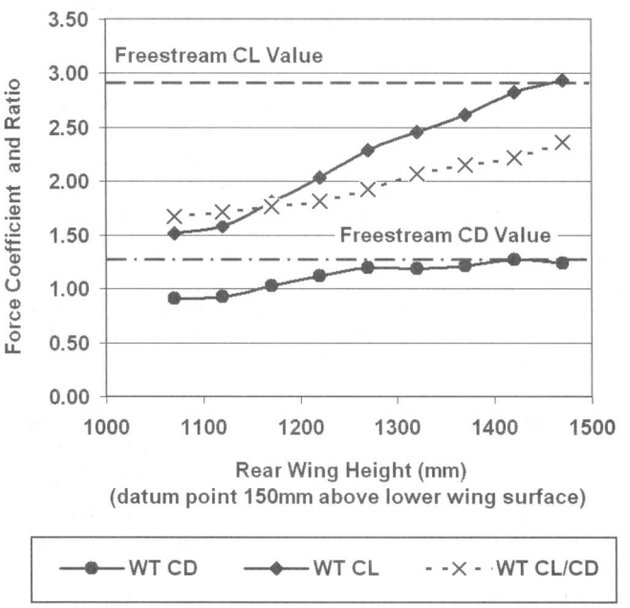

Figure 10: Rear wing (only) measured force coefficients (and lift to drag ratio) with car and driver in place versus rear wing height above ground (Dashed lines indicate measured free stream coefficients, representing infinite ground clearance), 30 degrees angle of attack.

The rear wing height sensitivity study showed major reductions in rear wing downforce due to the flow blockage and flow angularity caused by the car and driver. At the lowest tested rear wing height of 1.070 m, downforce was reduced by 48% compared with the free stream value, which can be considered the maximum value at infinite ground height. At the greatest height tested (1470mm) the rear wing achieved the same CL as in free-stream. It is interesting to observe how the drag of the wing plateaus much earlier than the downforce, and how the lift-to-drag ratio increases steadily with rear wing height. These results would suggest that the simplest way to increase the performance of a rear wing on a FSAE car is to increase its height above the car. They also suggest that a smaller, more efficient wing mounted high should provide both more downforce and less drag than a large wing mounted low. It should also be remembered that the size and height of the rear wing is ultimately limited by the amount of downforce that can be generated by the front wing for aerodynamic balance as described in [1].

WING IN 'GROUND EFFECT' INVESTIGATIONS

Due to the lack of a moving ground simulation in the Monash Wind Tunnel, a range of different methods were trialed to quantify and tune the performance of the front wing in ground effect. A brief description of these methods and some sample results will be presented here.

WING PRESSURE TAPPING TESTING

A pressure tapped front wing was constructed to record pressure contours over the upper and lower surfaces of the wing, and to provide a graphic and qualitative understanding of the wing's performance. Using software developed by Gilhome [25], the pressure point data is used to generate pressure contours which were then resolved into net drag and down forces. These resolved forces were correlated with measurements made simultaneously by the wind tunnel balance. The results presented here were used to benchmark the performance and accuracy of the system before on-track testing of the front wing in ground effect was commenced.

The pressure tapped wing was constructed with a total of 128 internal pressure taps. 120 of these taps were distributed over just one side of the wing (the right) for improved resolution. Tapping density was increased in regions of high expected pressure gradients in order to reduce interpolation errors. A further 8 taps were placed at strategic points on the left side of the wing to check that the assumption of symmetry was valid.

The experimental method and equipment used is described in detail by Gilhome [25]. A 128-channel Scannivalve system (ZOCENCL2100) was used to record 30 second samples at a rate of 200 Hz. The time averaged data was then used to develop full surface

pressure contours within the specified wing geometry, from which, downforce and drag forces were resolved. The tubing was routed back to the Scannivalve via the left hand side inner end plate to minimise interference with the flow on the right hand side where the vast majority of taps were located.

This system of pressure measurement and force interpolation was trialed in the wind tunnel using the free stream rig and compared with values measured simultaneously by the tunnel force balance. An example of the pressure contours are shown below (Fig. 11).

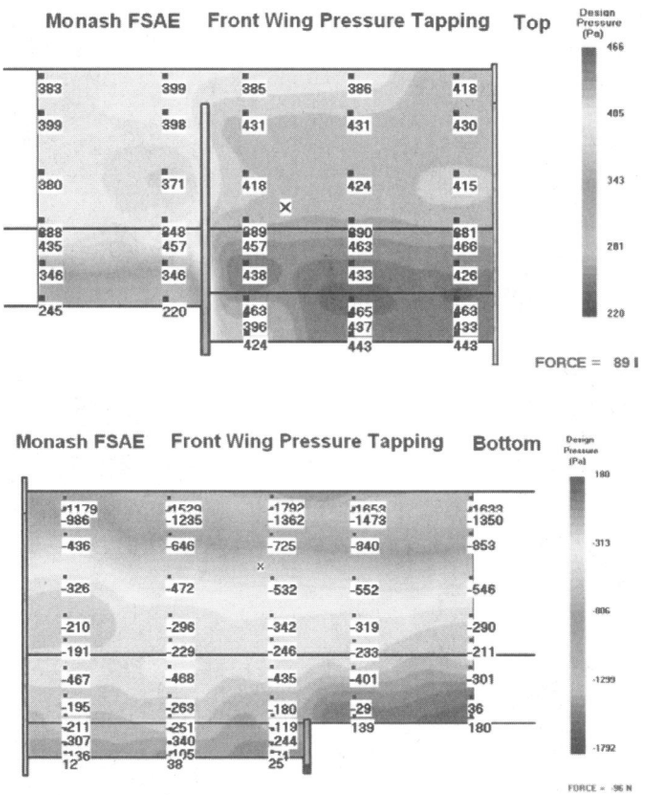

Figure 11: Example front wing pressure contour, free-stream flow, 16.7 m/s: Top – Right side, upper surface of the wing, Lower – Right side, bottom surface of the wing. Measurement locations and pressures (Pa) shown. 'X' marks force centroid.

A correlation plot featuring comparison of all the wind tunnel measured downforce, and pressure interpolated downforce, is shown below (Fig. 12). The four groups of dots correspond to different measurement speeds (20, 40, 60, 80 km/h). Different overall wing angle of attack settings provide the variations within each group.

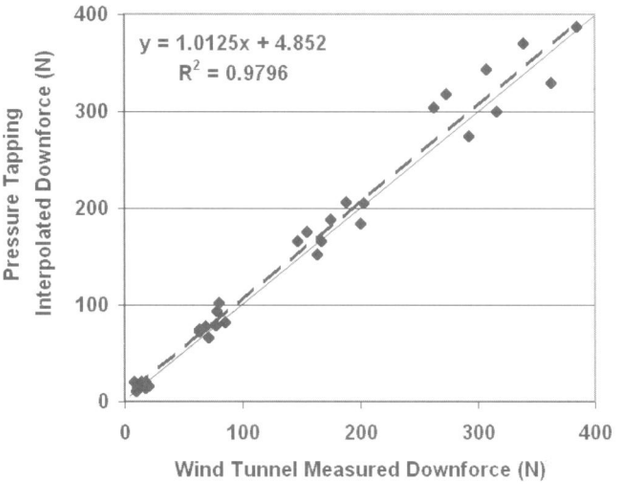

Figure 12: Correlation of pressure tapping interpolated downforce with wind tunnel measured downforce. Line of best fit (Dashed) shown, line of best fit equation and R^2 value provided on graph.

The slightly higher forces predicted by the pressure tapping (evidenced by the formula for the line of best fit shown on the graph) can be partially attributed to effect of the tubing on the wind tunnel measured values. The 128 tubes which exit on the left side of the wing would result in increased drag and reduced downforce as measured by the tunnel balance.

The scatter in the results indicated that further refinement and testing of the system was required to be able to choose the optimum wing setting from data recorded on track. Even still, the pressure tapping method is the only experimental method trialed which returns a qualitative understanding of the how the different regions of wing are performing and which areas are contributing to the generation of downforce. For this reason on-track, ground effect testing with this pressure tapped wing is planned for the near future.

FULL CAR 'SYMMETRY PLANE' TESTING

A full car 'symmetry plane' testing technique was another method used to investigate the performance of the front wing in ground effect. The principle of symmetrical testing has been proposed as a means of simulating a moving ground condition [5, pg 76]. It requires the test vehicle is effectively 'mirrored' in a plane of symmetry about the ground (Fig. 13).

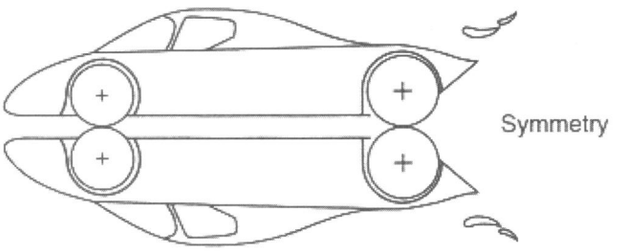

Figure 13: Example 'symmetry plane' test configuration, after Katz [5].

With reference to this technique Katz [5] states that;

"The basic idea here is that the symmetry line dividing the two identical models is a streamline. Therefore, the ground simulation is automatically obtained. Of course both models should be exactly the same (including the changes during the test)..."

Further analysis of this technique reveals that it is not quite so simple. Unlike a true moving ground simulation, the streamline created by the symmetry plane is not constrained to move at ground speed, which means that it may actually speed up or slow down due to the influence of the car or wing geometry. Depending on the relationship between the ground speed and the local flow field, this could result in a considerable change in the velocity profile, and hence the forces generated at the wing or vehicle surface.

Secondly, this technique assumes the existence of a streamline, which in turn assumes smooth, attached air flow. In practice, race cars have many turbulent regions with separated flow, for example, the wake behind the front wheels. Other parts of the car such as the front wing endplates may be designed specifically to induce strong vortices which may interact across the imagined plane of symmetry in a non-realistic and unrepresentative manner.

With these factors in mind, it was decided to construct a symmetry plane test rig to specifically look at performance of the front wing. The Monash 2004 car was used in this test because a near identical, carbon tub outer skin was available for use as the 'mirrored' car. The pressure tapped wing was used to 'mirror' the existing front wing. Stands were made to lift the 2004 car 1.5 meters in the air, below which the 'mirror' body work and 'mirror' front wheels were positioned. Because the force acting on only one of the front wings was to be measured, modeling of downstream components including the driver, engine bay and rear wing was neglected.

Both the upper and lower wings were fitted with specialized endplates allowing height adjustment in 15 mm increments and 2.5 degree angular increments. The mounts for the upper wing were attached to load cells on the floor of the tunnel to enable the download from this wing to be recorded. These load cells were calibrated using weights stacked on the wing. The effect of drag on the wing, which results in a bending moment at the load cells was also checked and found to be minimal. Photographs of the rig are shown in Figure 14.

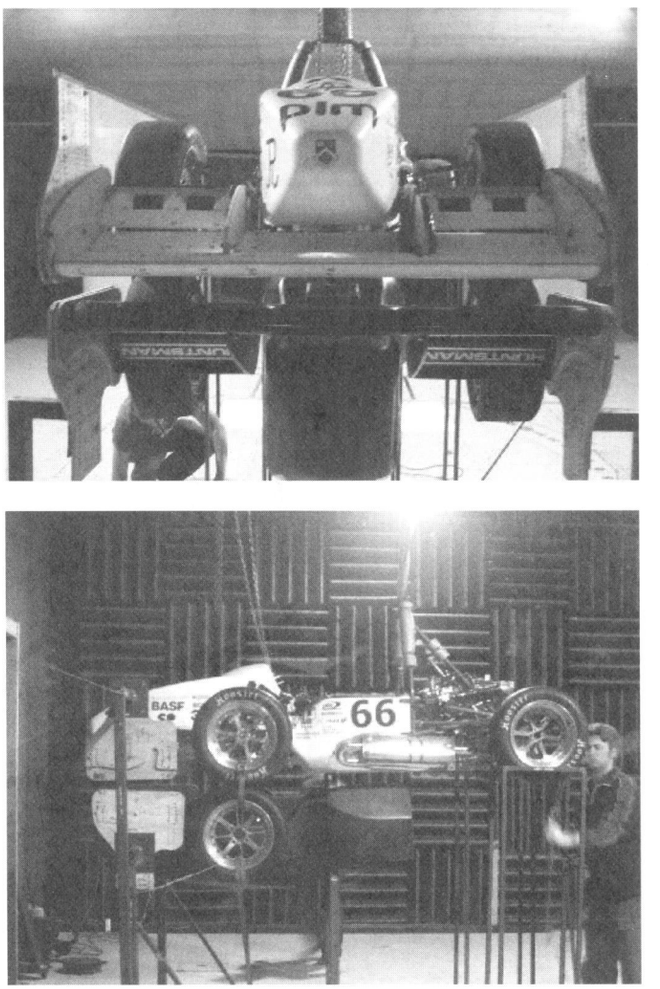

Figure 14: Full scale 'symmetry plane' test rig. Top: Front view, Bottom: Side view.

Achieving acceptable levels of symmetry between the two front wings proved difficult and limited the amount of quality data gathered from this test. An example of the results from this testing are shown below (Fig. 15). 2D CFD predictions for the same wing operating in ground effect (with no wheels or car) are provided for comparison.

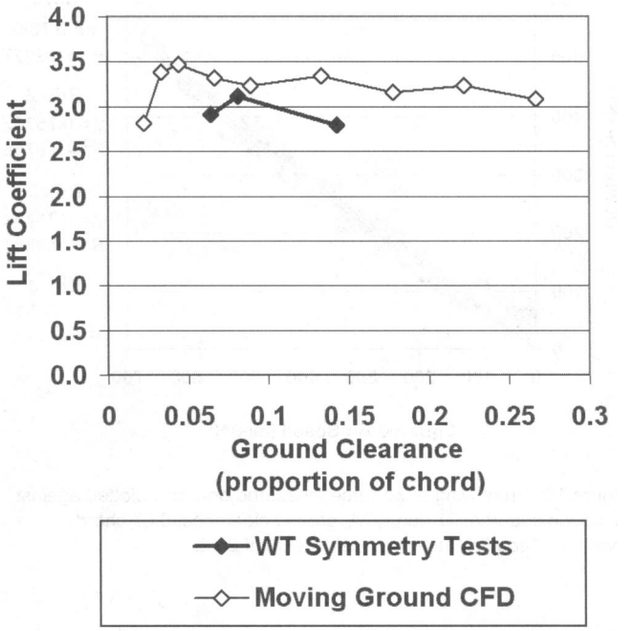

Figure 15: Wind tunnel symmetry rig measured front wing lift coefficients versus ground clearance for wing angle of attack 22 deg (Moving ground 2D CFD predictions provided for comparison).

As expected, these results were lower than predicted by the two dimensional CFD analysis due to:

- The shortened second flap, the centre third of which is permanently removed to enable the wing to clear the nose cone (Fig. 14); and
- The blockage and interference effects caused by the vehicle and, in this case, the stationary front wheels.

Further testing using the symmetry rig examined the effect of adding a 45 mm foot plate to the outside lower edge of the endplates. Such a flap is designed to help prevent flow migrating from the outside of the endplate, underneath into the low pressure region developed by the wing. Tests at a range of ground heights and wing angles of attack showed significantly improved downforce (8%) from the use of such a flap. Unfortunately, because such a flap is considered part of the wing, it must be located within the maximum allowable envelope for wings defined by the rules [2], and illustrated in [1]. This means that wing span must be reduced by a corresponding amount. Tests using different span wings suggested that a 13% loss in downforce would result from the required 90 mm reduction in wing span, and result in a net loss in downforce for this sized foot plate. Although not tested, it is thought that a smaller foot plate, in the order of 20 mm, might result in a net downforce gain.

FRONT WING ON TRACK TESTING

A strain-gauged front wing mount was constructed to log front wing downforce on the track. This mount consists of two 4-bar linkages in parallel with long, equal length upper and lower links. This allowed the wing one degree of freedom, vertical translation. Wing angle of attack was adjusted by substituting pre-made inner endplates. The forward vertical links on the 4-bar were connected to the outboard end of the top wishbone by a tie rod, so that wing movement was directly proportional to the displacement of the front wheels. Using this linkage the wing did not significantly change incidence angle or ride height during straight line acceleration or braking. The tie rod was designed to operate in tension only and was constructed from a turnbuckle in series with a wire cable and a strain gauged aluminium tube that acted as a load cell. The slender cable prevented the tie rod from reacting compressive loads, and acted to mechanically filter the downforce during cornering by removing the force couple. The turnbuckle also allowed ride height adjustment. The aluminum tubes in the tie rod were instrumented with 350ohm strain gauges and inclined in two planes to give the best practical downforce resolution. The strain gauges were in full bridge configuration to cancel any bending moments and to compensate for temperature effects. A pitot tube, connected to a Honeywell differential pressure sensor was used to log the air speed and account for differences in the atmospheric wind.

A CAD drawing and photograph of the final design is shown below (Figs. 16 and 17).

During testing calibration weights were added at the beginning and end of each run to allow offset and scaling errors to be compensated for, in post analysis. A reference plane was used to set the ride height and each test run was repeated four times, against and with the wind (if any). Each calibration and run was exported to a spreadsheet for analysis and correction of the individual offsets by linear interpolation. The scaling from the calibration runs was then applied to correct the logged data. The corrected data was then plotted against air speed squared and a linear regression performed on the data set. The least squares fit returned the v^2 coefficient for each angle of attack and ride height setting, allowing lift coefficients to be calculated.

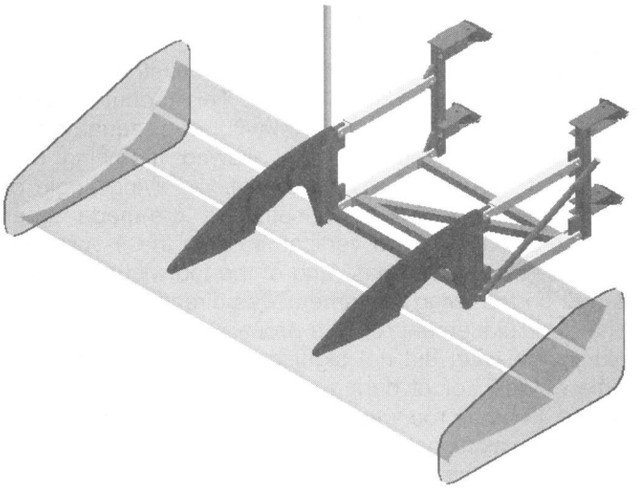

Figure 16: CAD design of the parallel linkage system for measuring downforce on the front wing. Tie rod links attach to outboard wishbone pick-ups.

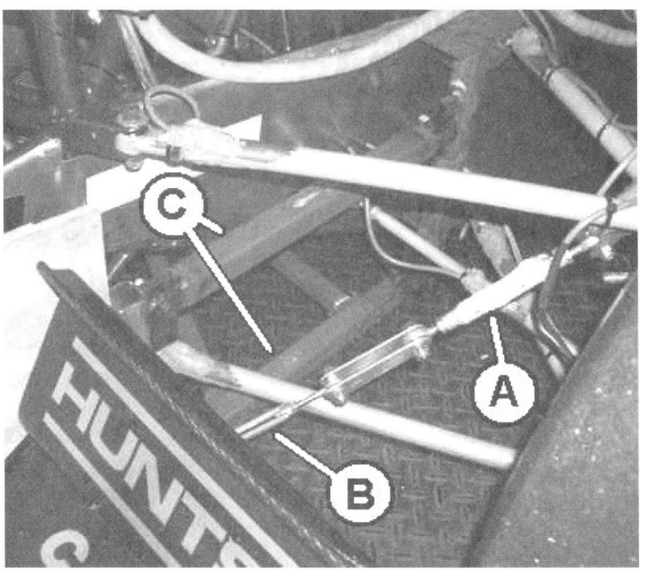

Figure 17: Photo of the parallel linkage system for measuring downforce on the front wing. A: strain gauged link shown attached to the outboard top wishbone, B: turnbuckle for adjustable ride height, C: parallel linkages.

An example of the raw data for a single wing setting, plotted against the air speed squared is shown in Figure 18 below. Equations and R^2 values are given for the linear regressions of each of the four runs. The coefficient of variation (standard deviation divided by mean) between the four separate runs was 3%.

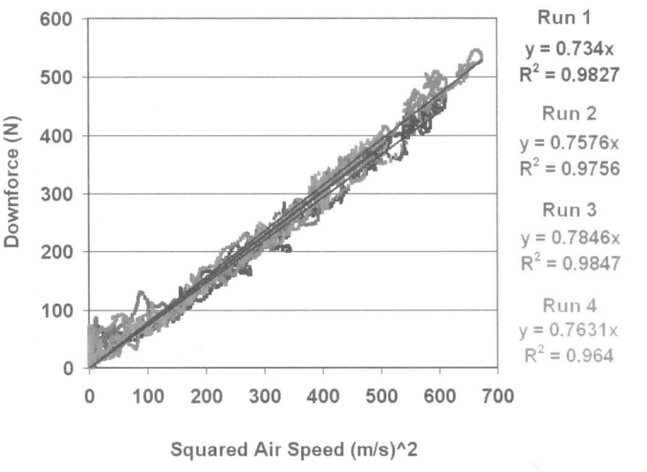

Figure 18: Front wing down force measured on-track, plotted against air speed squared, 27 deg AOA, ground clearance: 0.07 chord. Average v^2 coefficient of 0.76 yields a CL of 2.42.

Front wing lift coefficients for all tested angles of attack and ground clearances are plotted in Figure 19 below.

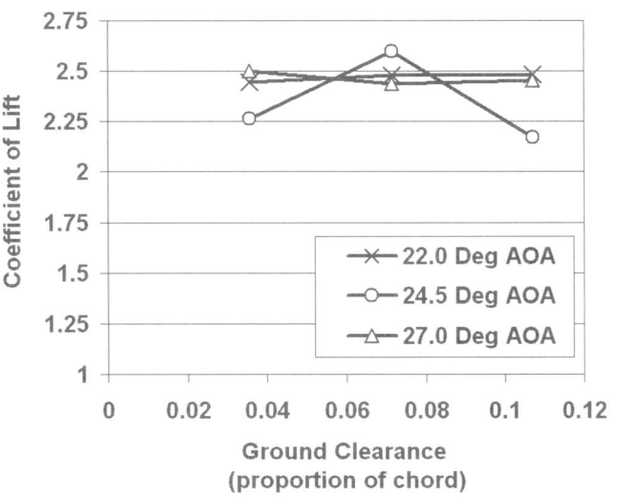

Figure 19: Front wing on-track measured coefficients of lift versus ground clearance for a range of angles of attack.

These results showed a small amount of variation in the front wing lift coefficients with changing angle of attack and ground clearance. These values were also slightly lower than those measured using the symmetry plane testing, possibly due to the effect of rotating wheels and slight differences in the car bodies (2003 car was used for on-track testing, 2004 for symmetry rig). The trends observed also differed considerably compared to the initial two-dimensional CFD study, most likely because of the front wheel and nose cone interactions which were not accounted for in the 2D CFD.

FINAL RESULTS

The net measured downforce and drag of the 2003 Monash Formula SAE car was:

- Car Coefficient of Lift: -2.57
- Car Coefficient of Drag: 1.33
- Car Frontal Area: 1.35 m^2

This result uses the downforce values measured on-track for the front wing in ground effect, in combination with the downforce and drag of the car and rear wing as measured in the wind tunnel.

CONCLUSIONS

In this study the following conclusions are drawn with respect to the development of an aerodynamics package for Formula SAE:

- Two-dimensional CFD can be useful for initial wing profile development, but is not always a reliable method for estimating their performance in close proximity to the car. The angles of attack for maximum CL were generally under predicted by 2D CFD, with this error increasing with smaller prototype wing aspect ratios. Three-dimensional CFD modeling, wind tunnel testing or on-track data logging is therefore recommended to confirm wing performance.

- The downforce generated by a high lift, low aspect ratio rear wing is particularly sensitive to the flow blockage and angularity caused by the car. Increasing the rear wing height was shown to be a simple way to increase rear downforce for only a minor drag penalty. A high mounted rear wing with a high lift to drag ratio is therefore recommended.

- High lift front wings operating in ground effect can cause the majority of the cooling airflow to be deflected above traditional side pod mounted heat exchangers. Redesign or relocation of the cooling system or ducting may be required to ensure adequate cooling performance.

- The performance of a high lift front wing in ground effect is dependant on a complex interaction between angle of attack, ground clearance and blockage caused by the car nose and front wheels. 3D CFD, moving ground wind tunnel or on-track testing is needed to ensure that the best performance is obtained.

- The method of pressure tapping and force interpolation was shown to predict downforce values within 10% of those measured. The qualitative picture this method provides makes it an attractive option for the study of wings (and other devices) in ground effect and complex aerodynamic environments.

- The method of full-scale symmetry testing was found to be a viable (but labor intensive) method of simulating a moving ground in scenarios where the airflow is generally smooth and attached. Extreme care must be taken to ensure that symmetry is satisfied.

- The method of strain gauging a front wing mount was found to be successful provided that the ambient wind speed is logged. Of the three methods tested for measuring the performance of a front wing in ground effect, this appeared to be the easiest and most accurate.

REFERENCES

1. Wordley, S.J., and Saunders, J.W., ***Aerodynamics for Formula SAE: Initial Design and Performance Prediction***, SAE Paper 2006-01-0806, 2006.
2. SAE, ***2005 Formula SAE Rules, US Comp Edition***, Society of Automotive Engineers, USA, 2004.
3. UIUC,***UIUC Airfoil Coordinates Database***, http://www.ae.uiuc.edu/m-selig/ads/coord_database.html
4. McBeath, S., ***Competition Car Downforce***, Haynes Publishers, Somerset, 1998
5. Katz, J., ***Race Car Aerodynamics***, Bentley Publishers, USA, 1995.
6. Zerihan, J. and Zhang, X., ***Aerodynamics of a Single Element Wing in Ground Effect***, Journal of Aircraft, Vol 37, No. 6, pp 1058-1064, 2000.
7. Zhang, X., and Zerihan, J., ***Aerodynamics of a Double Element Wing in Ground Effect***, AIAA Journal, Vol. 41, No. 6, pp 1007-1016, 2003.
8. Liebek, R. H., ***Design of Subsonic Airfoils for High Lift***, Journal of Aircraft, Vol. 15, No. 9, pp. 547-561, 1978.
9. Gopalarathnam, A., Selig, M.S. and Hsu, F., ***Design of High-Lift Airfoils for Low Aspect Ratio Wings with Endplates***, AIAA Paper 97-2232, 1997
10. Lin, C., Saunders, J.W., Watkins, S., and Mole, L., ***Increased Productivity – Use Specific Dissipation to Evaluate Engine Cooling***, Topics in Vehicle Aerodynamics, SP-1232, SAE pp 67-79, 1997.
11. Hucho, W., ***The aerodynamics of road vehicles***, Butterworths Publishers, London, 1965.
12. Razenbach, R., and Barlow, J.B., ***Two-Dimensional Airfoil in Ground Effect, An Experimental and Computational Study***, SAE Paper 942509, 1994 Motorsport Engineering Conference Proceedings, Vol 1, pp. 241-249, 1994
13. Razenbach, R., and Barlow, J.B., ***Cambered Airfoil in Ground Effect – An Experimental and Computational Study***, SAE Paper 960909, 1996

Motorsport Engineering Conference Proceedings, Vol 1, pp. 269-276, 1996
14. Ross, J.C., Storms, B.L., and Carrannanto, P.G., ***Lift-Enhancing Tabs on Multielement Airfoils***, Journal of Aircraft, Vol 32, No. 3, pp 649-655, 1995.
15. Jasinski, W.J., and Selig, M.S., ***Experimental Study of Open-Wheel Race-Car Front Wings***, SAE Paper 983042, 1998.
16. Shew, J.E., and Wyman, L.R., ***Race Car Front Wing Design***, Paper No. AIAA-2005-139, AIAA Aerospace Sciences Meeting and Exhibit, Reno, USA, 2005
17. Coiro, D.P., et al, ***Experiments and Numerical Investigation on a Multi-Component Airfoil Employed in a Racing Car Wing***, SAE paper 970411, Topics in Vehicle Aerodynamics, pp. 221-231, 1997.
18. Petrone, N., et. al, ***Acquisition and Analysis of Aerodynamic Loads on Formula 3 Racing Car Wings using Dynamometric Load Cells***, SAE Paper 2002-01-3331, 2002.
19. McKay, N.J. and Gopalarathnam, A., ***The Effects of Wing Aerodynamics on Race Vehicle Performance***, SAE Paper 2002-01-3294, 2002.
20. Kellar W.P., Pearse S.R.G., Savill A.M., ***Formula 1 car wheel aerodynamics***, Sports Engineering, Vol. 2, No. 4, November 1999, pp. 203-212.
21. Milliken, W.F., and Milliken, D.L., ***Race Car Vehicle Dynamics***, SAE International, 1995.
22. Ping, C., ***Shift-time Limited Acceleration: Final Drive Ratios in Formula SAE***, SAE Paper 2004-01-3554, 2004
23. Case, D., ***Formula SAE: Competition History 1981-2004***, Society of Automotive Engineers, USA, 2005.
24. Gilhome, B. G., Saunders, J. W. and Sheridan, J., ***Time Averaged and Unsteady Near-Wake Analysis of Cars,*** 2001-01-1040 in SAE SP, Proc. SAE Congress, Detroit, March, 2001.
25. Gilhome B.G., Saunders J.W. ***The Effect of Turbulence on Peak and Average Pressures on a Car Door***, SAE Paper 2002-01-0253, 2002.

CONTACT

Scott Wordley:

Email: scott.wordley@eng.monash.edu.au

Website: http://www-personal.monash.edu.au/~fsae/

APPENDIX

Schematic of the Monash Wind Tunnel: